

pubs.acs.org/acssensors Article

Genetically Encoded RNA-Based Bioluminescence Resonance Energy Transfer (BRET) Sensors

Lan Mi, Qikun Yu, Aruni P. K. K. Karunanayake Mudiyanselage, Rigumula Wu, Zhining Sun, Ru Zheng, Kewei Ren,* and Mingxu You*



Cite This: https://doi.org/10.1021/acssensors.2c02213



ACCESS Metrics & More

BRET "OFF"

BRET "ON"

Target binding aptamer

Target Fluorogenic RNA

Substrate

Dye

Nanel US

ABSTRACT: RNA-based nanostructures and molecular devices have become popular for developing biosensors and genetic regulators. These programmable RNA nanodevices can be genetically encoded and modularly engineered to detect various cellular targets and then induce output signals, most often a fluorescence readout. Although powerful, the high reliance of fluorescence on the external excitation light raises concerns about its high background, photobleaching, and phototoxicity. Bioluminescence signals can be an ideal complementary readout for these genetically encoded RNA nanodevices. However, RNA-based real-time bioluminescent reporters have been rarely developed. In this study, we reported the first type of genetically encoded RNA-based bioluminescence resonance energy transfer (BRET) sensors that can be used for real-time target detection in living cells. By coupling a luciferase bioluminescence donor with a fluorogenic RNA-based acceptor, our BRET system can be modularly designed to image and detect various cellular analytes. We expect that this novel RNA-based bioluminescent system can be potentially used broadly in bioanalysis and nanomedicine for engineering biosensors, characterizing cellular RNA—protein interactions, and high-throughput screening or *in vivo* imaging.

KEYWORDS: bioluminescence resonance energy transfer, fluorogenic RNA aptamers, bioluminescent sensors

Genetically encodable fluorescent and bioluminescent sensors are the most widely used tools for live-cell imaging and detection of various biomolecules and signaling events. While fluorescent molecules rely on the absorption of excitation light to reemit photons, bioluminescence can produce light directly through chemical reactions. Compared to bioluminescence, although fluorescence signals are often brighter, the requirement of excitation light may cause higher background, photobleaching, and phototoxicity. Bioluminescence and fluorescence have thus been frequently used as complementary tools for studying cellular processes.

A wide variety of protein-based fluorescent and bioluminescent sensors have been developed for both cellular and *in vivo* studies. ^{5–9} In contrast, only recently, RNA-based genetically encodable fluorescent sensors began to be engineered for intracellular measurement. ¹⁰ The major advantages of these RNA-based sensors include their high sensitivity, modularity, and ease of engineering and evolution. As a result, different RNAs, proteins, and small-molecule analytes can be detected and imaged by these RNA-based

fluorescent sensors.^{11–14} On the other hand, RNA-based bioluminescent sensors remain largely underdeveloped. RNA-based genetic regulators can induce bioluminescence signals by controlling the cellular expression of luciferase reporters.^{2,11,15} However, these RNA nanodevices can rarely be used as biosensors for the real-time detection or monitoring of cellular target analytes.

In this project, our goal is to design a novel type of genetically encoded RNA biosensors that can produce real-time bioluminescence signals inside living cells without the use of excitation light. Our strategy is based on the modulation of bioluminescence resonance energy transfer (BRET) between a

Received: October 11, 2022 Accepted: December 27, 2022



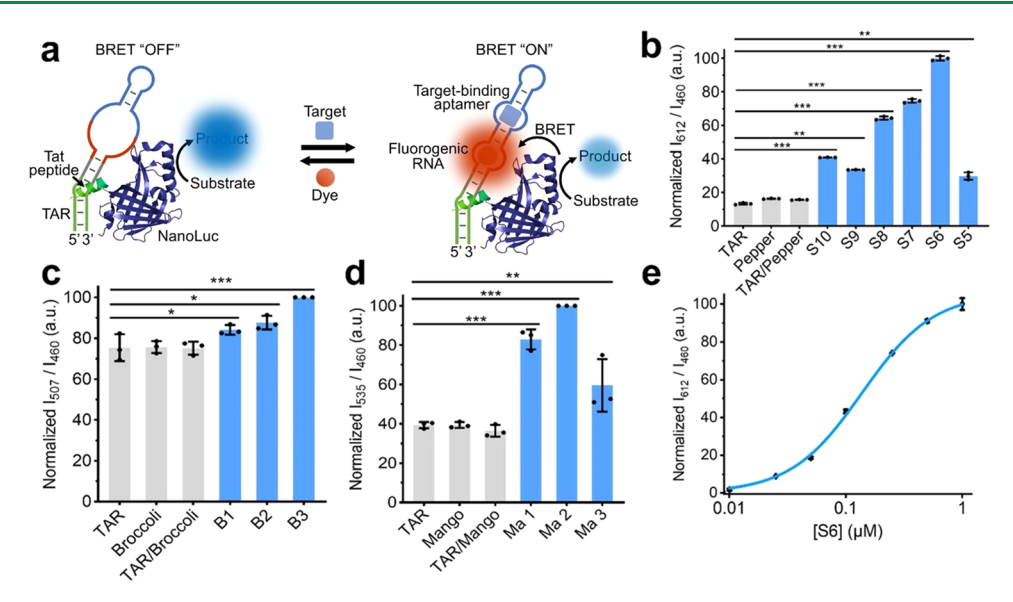


Figure 1. (a) Schematic illustration of a modular BRET sensor system based on TAR—Tat interaction-induced energy transfer between NanoLuc/substrate complex and fluorogenic RNA (FR)/dye pairs. The target binding to the aptamer region induces the folding of fluorogenic RNA to bind the dye molecule. While it is worth mentioning that data shown in the rest of Figure 1 was measured using RNA constructs without containing a target-binding aptamer region. (b) I_{612}/I_{460} (acceptor/donor) ratiometric BRET signal was measured at 25 °C in a solution containing 100 nM t-NLuc, 1 μM RNA, 5 μM HBC620, and 5 mM Mg^{2+} at 30 s after adding the 1% (v/v) furimazine substrate. S5–S10 represent the t-NLuc/TAR-Pepper construct containing 5–10-base-pair-long linkers, respectively. The mixture of t-NLuc with TAR, Pepper, and their simple mixture (TAR/Pepper) acted as the negative controls. (c, d) BRET efficiency of the Broccoli- and Mango II-based t-NLuc/RNA construct with different linker lengths (named as B1, B2, and B3 and Ma1, Ma2, and Ma3). The I_{507}/I_{460} and I_{535}/I_{460} ratiometric signals were measured in a solution containing 100 nM t-NLuc and 1 μM RNA at 25 °C in the presence of 20 μM DFHBI-1T or 1 μM TO1-biotin. The mixture of t-NLuc with TAR (without Broccoli or Mango II), Broccoli, Mango II (without TAR conjugation), or simple mixtures of Broccoli/Mango II and TAR (i.e., TAR/Broccoli and TAR/Mango) were used as negative controls. (e) Normalized I_{612}/I_{460} BRET signal of the t-NLuc/S6 construct after mixing 100 nM t-NLuc with different concentrations of S6 RNA. Shown are the mean and standard deviation (SD) values from three independent replicates. *p < 0.05, **p < 0.01, ***p < 0.001 in two-tailed Student's t-test.

donor luciferase enzyme and an acceptor fluorescent RNA species (Figure 1a). An important advantage of BRET-based biosensors is that they can provide ratiometric signals to allow real quantitative measurement of target analytes. ^{7,16}

Several protein-based BRET sensors have been previously developed to detect different cellular target molecules or protein—protein interactions.^{2,17,18} In these sensors, the ratiometric BRET signals are generated between an adjacent pair of luciferase and fluorescent protein. The brightness and stability of the luciferase and substrate are critical to the sensitivity of the BRET sensors.^{18,19} For example, the NanoLuc luciferase (NLuc) has been popularly used as a BRET donor due to its small size, high catalytic efficiency, and stability.^{20,21}

To develop an RNA-based BRET system, herein, we chose to continue using luciferase (e.g., NLuc) as the donor moieties but will replace the fluorescent protein acceptors with fluorogenic RNA (FR) aptamers. FR aptamers are single-stranded RNAs that can bind and activate the fluorescence of corresponding small-molecule dyes. ^{22,23} We and others have previously demonstrated that these FRs can be engineered into modular fluorescent sensors for the sensitive imaging of various cellular targets. ^{11–14,24–29} We speculate that once our RNA-based BRET platform is established, these existing fluorescent RNA sensors can be readily converted to generate target-specific bioluminescence signals.

Herein, we will report the design and validation of the first RNA-based genetically encodable BRET system based on natural RNA-protein interactions. We have further incorporated modular FR sensors to engineer bioluminescent probes for the detection of different small-molecule analytes inside

living cells. With the development of this new type of RNA-based BRET sensors, a broad range of cellular target analytes, as well as RNA-protein interactions, can be potentially imaged and quantified *in vitro* or even *in vivo*.

■ EXPERIMENTAL SECTION

Chemicals and Reagents. All of the chemicals were purchased from Sigma or Fisher Scientific unless otherwise noted. Furimazine (Nano-Glo Luciferase Assay) was purchased from Promega (Madison, WI). All of the RNA structures were simulated and designed using Mfold online software and all of the RNA sequences used in this project are listed in Table S1. DNA oligonucleotides were synthesized and purified by the W.M. Keck Oligonucleotide Synthesis Facility (Yale University School of Medicine) or Integrated DNA Technologies (Coralville, IA). The stocks were dissolved at 100 μ M concentration in 10 mM Tris-HCl and 0.1 mM ethylenediaminetetraacetic acid (EDTA) at pH = 7.5 and stored at -20 °C. Doublestranded DNA template/nontemplate strands for in vitro transcription were prepared via polymerase chain reaction (PCR) amplification using an Eppendorf Mastercycler. The PCR products were purified and cleaned using a Monarch PCR & DNA cleanup kit (New England BioLabs, Ipswich, MA). RNAs for the in vitro test were transcribed using a HiScribe T7 high-yield RNA synthesis kit (New England BioLabs, Ipswich, MA) and then column-purified. These RNA strands were prepared in aliquots and stored at −20 °C for immediate usage or at -80 °C for long-term storage. All of the DNA/RNA concentrations were measured using a NanoDrop One UV-vis spectrophotometer.

Bioluminescence and Fluorescence Measurement. All of the *in vitro* bioluminescence and fluorescence measurements were conducted using a PTI fluorometer (Horiba, New Jersey, NJ) or a SpectraMax M2 multimode microplate reader. Fluorescence assays were conducted in a homemade buffer consisting of 40 mM *N*-(2-

hydroxyethyl)piperazine-N'-ethanesulfonic acid (HEPES), 100 mM KCl, 0.1% dimethyl sulfoxide (DMSO), and 1–5 mM MgCl₂ at pH = 7.5. Here, 1 μ M RNA and 5 μ M HBC620 (or 20 μ M DFHBI-1T for Broccoli or 1 μ M TO1-biotin for Mango II) were used for these measurements at 25 °C. Bioluminescence assays were performed either in the same homemade buffer or a NanoBuffer (Promega Nano-Glo Luciferase Assay), with the addition of 100 nM t-NLuc and 1 μ M RNA and their corresponding dye. All of these samples were first mixed and incubated at 25 °C for 30 min before taking the measurement. Right after the addition of 1% (v/v) furimazine, the BRET signals of each sample were collected at 460 nm (donor) and 612 nm (Pepper acceptor), 507 nm (Broccoli acceptor), or 535 nm (Mango II acceptor) without excitation. All of the analyzed data were plotted using Origin software.

Vector Construction. The DNA sequence of t-NLuc was first PCR amplified from a mini-CMV-NLuc-tDeg plasmid¹⁵ (gift from the Jaffrey Lab). The amplified t-NLuc sequence was then cloned into a pETite vector containing His tag for protein purification and in vitro characterization. For intracellular bioluminescent detection, sequences containing both a T7 promoter and terminator were cloned into a pETDuet vector. The t-NLuc-His tag was double-digested with NdeI and XhoI restriction enzymes (New England BioLabs), and the RNA sensor region was digested with SgrAI and SacII restriction enzymes. After gel purification, the digested vector was ligated with a similarly digested DNA insert using a T4 DNA ligase (New England BioLabs). The preparation of t-NLuc under the lac promoter in the reconstructed pETDuet plasmid was achieved following a similar procedure but was double-digested with SgrAI and SacII restriction enzymes. The ligated product was transformed into BL21 Star (DE3) cells (New England Biolabs) and screened based on their ampicillin resistance. All of these plasmids were isolated and confirmed by Sanger sequencing at Eurofins Genomics.

BRET Measurement in Bacterial Cells. BL21 Star (DE3) cells that express t-NLuc and RNA sensors were first grown in LB media at 37 °C until the optical density at 600 nm reached 0.4-0.5. Then, 1 mM isopropyl β -D-1-thiogalactopyranoside (IPTG) was added for a 2h induction. Afterward, 1 mL of cells was centrifuged for 2 min at a 5000g speed and then resuspended in 200 μ L of Dulbecco's phosphate-buffered saline (DPBS) or cell lysis buffer containing 5 μM HBC620. The target analyte was added into 100 μL of cell solutions and incubated for 30 min before adding furimazine. The bioluminescence and fluorescence signals were collected within a 96well plate using either a SpectraMax M2 multimode microplate reader or an IVIS SpectrumCT system. On the plate reader, the BRET signals were collected at both 460 and 612 nm wavelengths without excitation three times with calibration at 25 °C. All of the data were plotted with Origin software. In the IVIS SpectrumCT system, the BRET signals were collected at both 500 and 620 nm wavelengths without excitation. Images were taken with a 0.2-s exposure time, 1.5 cm subject height, and 13.3 cm² field of view. The processing of all images was accomplished using Fiji ImageJ software.

BRET Measurement in Mammalian Cells. HEK-293T cells were cultured in a DMEM medium supplemented with 10% fetal bovine serum, 100 unit/mL of penicillin, and 0.1 mg/mL of streptomycin at 37 °C in a 5% CO2 atmosphere. For microscope imaging, HEK-293T cells were seeded at a density of 2×10^5 cells per well into a poly-D-lysine-coated eight-chambered cover glass plate (Cellvis, C8-1.5H-N). For the plate reader experiment, these HEK-293T cells were seeded at a density of 5×10^4 cells per well into a 96well glass bottom plate (Cellvis, P96-1.5H-N). After overnight culturing, cells were transfected using the FuGENE HD transfection reagent (Promega) according to the manufacturer's instructions. To be more specific, 1 μ g of mini-CMV-t-NLuc was cotransfected with 1 μg of PAV-U6+27-Tornado-TAR or 1 μg of PAV-U6+27-Tornado-S6. After 24 h of transfection, cells were subcultured using a DPBS buffer containing 5 μ M HBC620 for 30 min. Fluorescence images were collected using a Nikon TiE inverted microscope with an Andor's Zyla sCOMS camera at 25 °C. Cells were excited with a 561 nm laser through a 40× oil objective. For the plate reader experiment, furimazine was added directly in each well before reading and the

donor luminescence signal at 460 nm and the acceptor signal at 645 nm were collected using a BioTek Synergy 2 plate reader.

RESULTS AND DISCUSSION

Design and Optimization of an RNA-Based BRET System. Inspired by previously reported BRET sensors that are regulated by protein-protein interactions, 7,30-33 we first wondered if natural RNA-protein complexes can also be used to control BRET signals. To test this idea, we chose to study a well-characterized bovine immunodeficiency virus interaction between a transactivation response (TAR) RNA and an arginine-rich Tat peptide. This TAR-Tat complex exhibits strong binding affinity (K_D , ~10 nM) and is naturally used to enhance transcriptional activation and elongation.³⁷ Guided by the structure of this RNA-peptide complex, 40,41 we fused an NLuc luciferase to the N-terminus of the Tat peptide (named "t-NLuc") and used it as the BRET donor (Figure 1a). Three types of FR aptamers, i.e., Broccoli, 42 Mango II, 43,44 and Pepper, 43,46 were respectively conjugated to the loop region of TAR and acted as the potential BRET acceptor (Table S1). This loop region of TAR has been shown to just play a structural role and thus can be swapped into different sequences without interfering with the formation of the TAR-Tat complex. 41,47 The three types of FRs were chosen based on their high brightness upon activating the corresponding dyes, i.e., DFHBI-1T, TO1-biotin, and HBC620. These FR/dye pairs can also cover a large spectral range, i.e., Broccoli/DFHBI-1T ($\lambda_{\rm ex}/\lambda_{\rm em}$, 472/507 nm), Mango II/TO1biotin ($\lambda_{\rm ex}/\lambda_{\rm em}$, 510/535 nm), and Pepper/HBC620 ($\lambda_{\rm ex}/\lambda_{\rm em}$, 572/612 nm).

Because the BRET efficiency strongly depends on the distance and orientation between the donor and acceptor modules, we next wanted to optimize these factors between NLuc and FRs. Instead of changing the peptide linker that connects Tat with NLuc, it is much easier to synthesize and adjust the RNA linker between TAR and FR aptamers. By simply altering the length of the RNA linker, considering the A-form helical conformation of the RNA duplex, we can finetune both the distance and orientation between NLuc and FRs. For example, in the case of the Pepper acceptor, 5-10-basepair-long linkers (named S5-S10, respectively) were synthesized and tested in vitro (Table S1). Our results indicated that the fusion of Pepper and TAR via these linkers will not influence the Pepper/HBC620 fluorescence signal (Figure S1a). While in the presence of t-NLuc, upon adding furimazine, the NanoLuc substrate, the BRET signals can indeed be observed but highly dependent on the length of RNA linkers (Figure S1b).

To compare the efficiency among these different BRET pairs, the bioluminescence ratios between the acceptor (e.g., I_{612} for Pepper) and donor (I_{460}) channels were determined. Measurement of these ratiometric I_{612}/I_{460} signals can minimize the influence of incubation time and substrate concentration on the bioluminescence readout (Figure S2). Our results showed that in the presence of S5–S10 RNA, a 1.2- to 7.2-fold increase in the I_{612}/I_{460} BRET signals was observed (Figure 1b). The maximum I_{612}/I_{460} ratiometric signal was detected with the t-NLuc/S6 complex. As a control, without linking TAR with Pepper, a minimal I_{612}/I_{460} signal was shown, indicating that the TAR–Tat interaction is required for the generation of strong BRET signals.

We have also measured the BRET efficiency of other t-NLuc/FR systems using Broccoli/DFHBI-1T or Mango II/

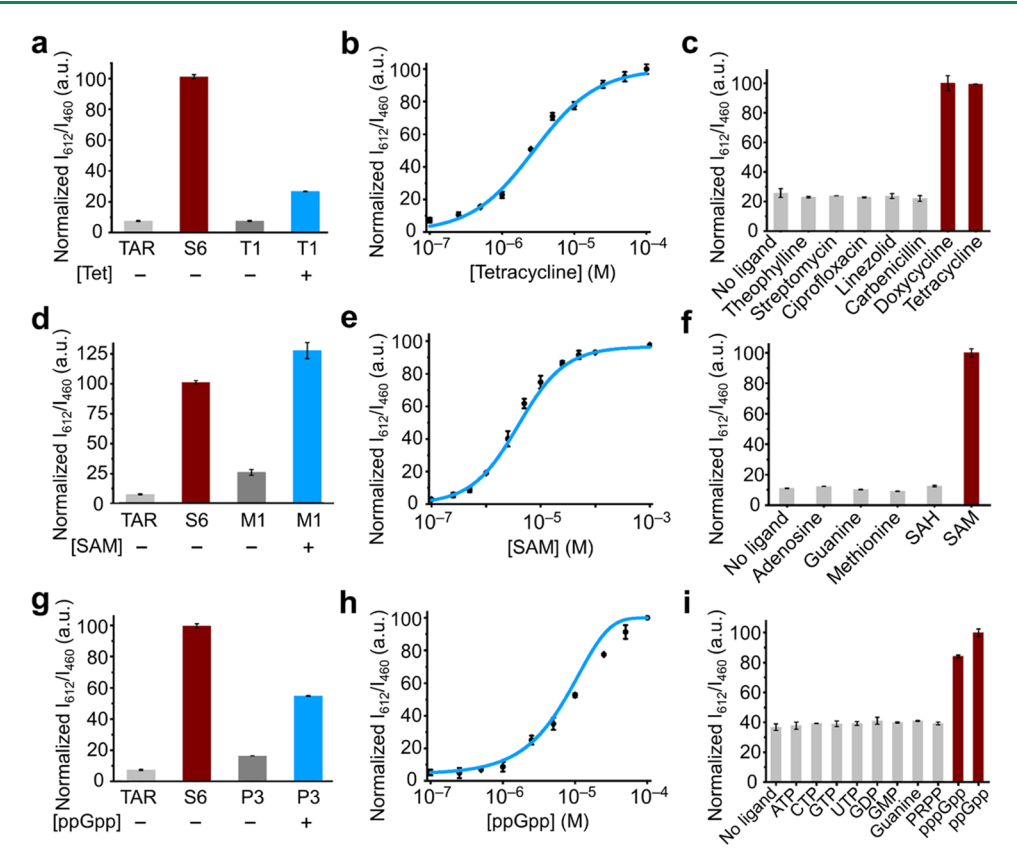


Figure 2. In vitro characterization of different RNA-based BRET sensors. The I_{612}/I_{460} ratiometric signals of the optimal (a) t-NLuc/T1 tetracycline sensor, (d) t-NLuc/M1 S-adenosyl methionine (SAM) sensor, and (g) t-NLuc/P3 guanosine tetraphosphate (ppGpp) sensor were measured in the presence or absence of 100 μM tetracycline (Tet), SAM, or ppGpp. The mixture of t-NLuc with TAR or S6 acted as a negative control and positive control, respectively. (b, e, h) Dose—response curve of the t-NLuc/T1 tetracycline sensor, t-NLuc/M1 SAM sensor, and t-NLuc/P3 ppGpp sensor after adding different amounts of tetracycline, SAM, or ppGpp. (c, f, i) Selectivity of the t-NLuc/T1 tetracycline sensor, t-NLuc/M1 SAM sensor, and t-NLuc/P3 ppGpp sensor was measured in a solution containing 100 μM counter ligands. The control was measured without adding ligands. All of these measurements were performed in a solution containing 100 nM t-NLuc, 1 μM RNA, and 5 μM HBC620 at 25 °C after adding the 1% (v/v) furimazine substrate. Shown are the mean and the standard error of the mean values from three independent replicates in each case.

TO1-biotin as the acceptor. After optimizing the linker lengths between TAR and FR (Table S1), the ratiometric BRET signals were determined at I_{507}/I_{460} and I_{535}/I_{460} , respectively. However, only up to 33% and 156% increase in the BRET signal was observed in the presence of Broccoli or Mango II acceptor, respectively (Figure 1c,d). Although these results indicated that different types of FRs can be potentially used to generate bioluminescence signals, considering the much larger signal enhancement and red-shifted emission spectra from the Pepper/HBC620 system, we decided to use the t-NLuc/S6 platform for the following studies.

To further optimize the BRET signals of this t-NLuc/S6 system, we studied the effect of Mg²⁺ concentration (Figure S3) and other buffer conditions (Figure S4). Magnesium ions can potentially influence the binding affinity of the TAR—Tat complex⁴⁷ as well as the folding of Pepper RNA.⁴⁵ Indeed, without adding Mg²⁺, a minimal I_{612}/I_{460} signal was observed (Figure S3). While at the physiological Mg²⁺ level (~2 mM),^{48,49} an ~11.0-fold increase in the I_{612}/I_{460} BRET signal was shown, indicating that t-NLuc/S6 may be potentially used under normal biological conditions. As we further increased the Mg²⁺ concentration from 2 to 20 mM, a gradual decrease in the I_{612}/I_{460} signal was detected, which may be due to the formation of other unwanted RNA tertiary structures.

In addition, we wondered if these BRET signals are indeed correlated with the concentrations of S6 RNA. To test this, we

mixed 100 nM t-NLuc with different amounts of S6 and measured their I_{612}/I_{460} ratiometric signals (Figure 1e). Our results indicated that a large concentration range (10–500 nM) of S6 can be distinguished based on their BRET signals. A half-maximal ratiometric intensity was reached after adding \sim 100 nM S6, *i.e.*, stoichiometrically equivalent to that of t-NLuc.

Development of RNA-Based BRET Sensors. After characterizing and optimizing the function of the t-NLuc/S6 system, we next asked if this platform can be further used to develop sensors for detecting target analytes. Inspired by the modular design of FR-based allosteric fluorescent sensors, 22 we wondered if RNA-based BRET sensors can also be engineered similarly by fusing target-binding aptamers into the S6 RNA (Figure 1a). In this case, upon the addition of target analytes, target-binding aptamers undergo structural changes to regulate the folding of Pepper RNA, *i.e.*, the BRET acceptor. Consequently, the I_{612}/I_{460} ratiometric BRET signal will be directly correlated with the amount of target analytes.

We realized that the P2 stem region of Pepper is sequenceindependent and thus can be potentially used to insert these target-binding aptamers. ⁴⁶ To test this design principle, we first developed BRET sensors for detecting tetracycline (Tet), a widely used antibiotic for fighting bacterial infections. ⁵⁰ Five different double-stranded transducers were designed to link the tetracycline aptamer into S6 (Figure S5 and Table S1). These

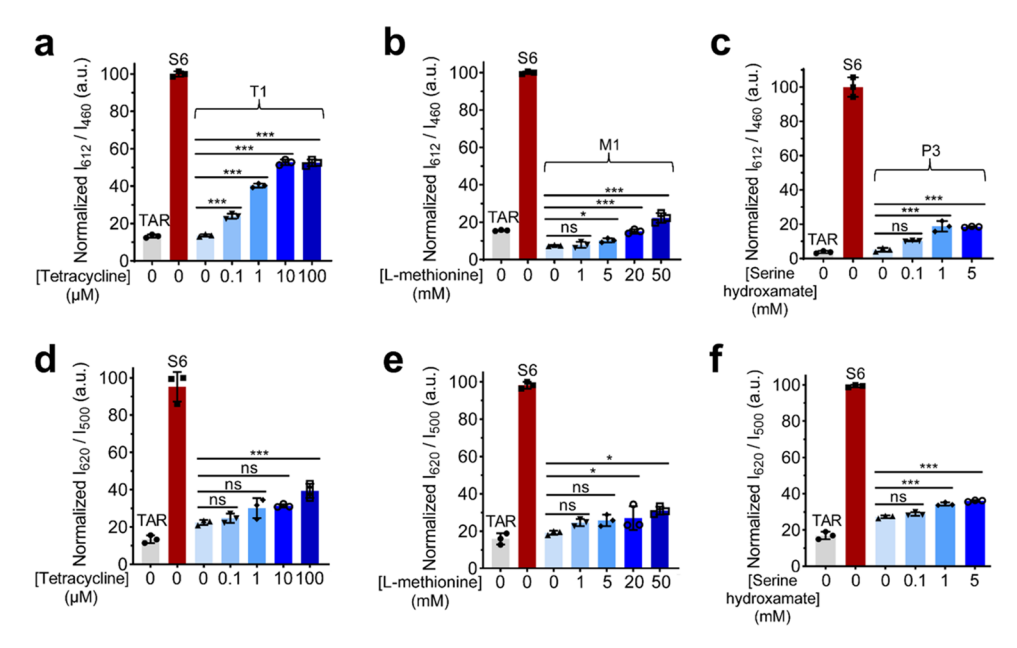


Figure 3. Target detection in living BL21 Star (DE3) *E. coli* cells with different RNA-based BRET sensors. The ratiometric signals of t-NLuc/T1 sensor-expressing cells in the presence of different amounts of tetracycline using (a) a plate reader (I_{612}/I_{460}) and (d) IVIS SpectrumCT (I_{620}/I_{500}) . The ratiometric signals of t-NLuc/M1 sensor-expressing cells in the presence of different amounts of L-methionine, a precursor for the cellular synthesis of SAM, using (b) a plate reader (I_{612}/I_{460}) and (e) IVIS SpectrumCT (I_{620}/I_{500}) . The ratiometric signals of t-NLuc/P3 sensor-expressing cells in the presence of different amounts of serine hydroxamate (SHX) for inducing bacterial starvation and ppGpp generation, using (c) a plate reader (I_{612}/I_{460}) and (f) IVIS SpectrumCT (I_{620}/I_{500}) . Cells expressing t-NLuc/TAR or t-NLuc/S6 acted as a negative control and positive control, respectively. The measurement was performed at 25 °C in the presence of 5 μ M HBC620 right after adding the 1% (v/v) furimazine substrate. Shown are the mean and SD values from three independent replicates. *p < 0.05, ***p < 0.001 in two-tailed Student's t-test; ns, not significant.

transducers were chosen because they have been previously applied to engineer modular RNA-based tetracycline sensors. Each of these sensor structures was further characterized *in silico* using Mfold online software. By measuring the I_{612}/I_{460} BRET signal of each RNA sensor in the presence or absence of 100 μ M tetracycline using a solution containing 1 μ M RNA and 100 nM t-NLuc, an optimal sensor (T1) was identified that exhibited a \sim 3.4-fold increase in the ratiometric BRET signal (Figures 2a and S5a).

A dose—response curve for tetracycline was further measured using this t-NLuc/T1 sensor (Figure 2b). The EC₅₀ value of this tetracycline-targeting BRET system was determined to be ~2.8 μ M. The t-NLuc/T1 sensor can be used for detecting a large concentration range (0.1–100 μ M) of tetracycline. As a control, the bioluminescent signals from either t-NLuc/TAR or t-NLuc/S6 were not affected by incubating with 100 μ M tetracycline (Figure S5b). To further test the target selectivity of this BRET sensor, we incubated 100 μ M theophylline, streptomycin, ciprofloxacin, doxycycline, linezolid, or carbenicillin with this t-NLuc/T1 sensor system (Figure 2c). As expected, a minimal I_{612}/I_{460} signal was shown, except for doxycycline, which belongs to the same tetracycline family and shares a quite similar four-ring structure as tetracycline. ⁵³

We wondered if this new RNA-based BRET sensor design can also be modularly used to develop sensors for different target analytes, such as S-adenosyl methionine (SAM), metabolite for methylation, transsulfuration, polyamine synthesis, ^{54,55} and guanosine tetraphosphate (ppGpp), signaling molecules involved in the bacterial response to stringent conditions. ^{56–58} Naturally existing RNA riboswitches that can selectively recognize SAM⁵⁹ and ppGpp^{60,61} have been

identified and used previously for engineering FR-based fluorescent sensors. $^{13,62}\,$

To convert these riboswitches into BRET sensors, we again focused on the design of transducer sequences between the aptamer domain of the riboswitch and the Pepper P2 stem region (Figure 1a and Table S1). In the presence of t-NLuc, after mixing these candidate RNA sensors with 100 μ M SAM or ppGpp, a 10.0-fold and 2.2-fold enhancement in the I_{612}/I_{460} ratiometric signal were observed for the optimal SAM (t-NLuc/M1) and ppGpp (t-NLuc/P3) sensors, respectively (Figures 2d,g and S5). Interestingly, the activated M1 sensor signal was even higher than that of S6, which is likely due to the different percentages of properly folded RNAs. As shown in Figure 1e, the intensities of BRET signals depend on the RNA concentrations, i.e., the concentrations of properly folded RNAs that can form the dye-binding pocket for generating BRET signals. We think that the SAM-induced folding of M1 sensors may actually generate a higher percentage of wellfolded RNAs than that of free S6 and, as a result, exhibit a higher BRET signal than S6. However, as expected, the I_{612} / I₄₆₀ signals of t-NLuc/TAR and t-NLuc/S6 controls were not affected after adding 100 μ M SAM or ppGpp (Figure S5). These optimized BRET sensors can be used to detect 1-100 μ M SAM and ppGpp, with an EC₅₀ value of 5.2 and 7.1 μ M, respectively (Figure 2e,h).

We next tested if these BRET sensors can retain the target selectivity of natural riboswitches. For this purpose, we incubated adenosine, guanine, methionine, and S-adenosylhomocysteine (SAH) with the t-NLuc/M1 sensor and ATP, CTP, GTP, UTP, GDP, GMP, and guanine with the t-NLuc/P3 sensor. None of these compounds affected the I_{612}/I_{460} signal of the BRET sensors (Figure $2f_{i}$). Indeed, the target

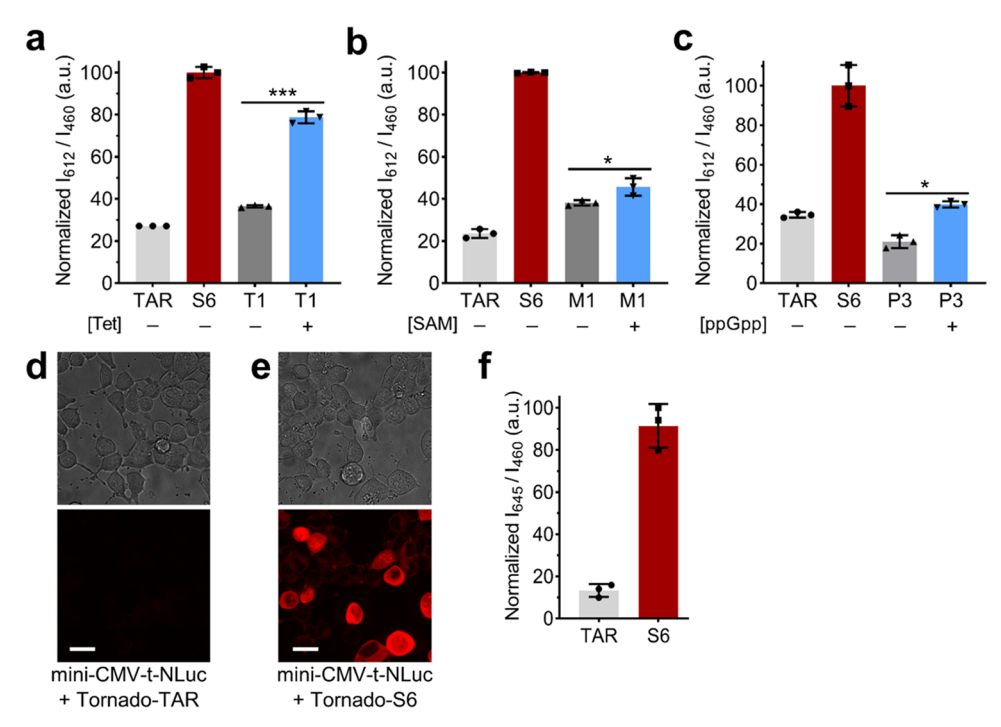


Figure 4. (a) I_{612}/I_{460} ratiometric BRET signals of genetically encoded t-NLuc/T1 sensors in BL21 Star (DE3) cell lysates in the absence or presence of additional 100 μM tetracycline. (b) I_{612}/I_{460} ratiometric BRET signals of genetically encoded t-NLuc/M1 sensors in BL21 Star (DE3) cell lysates in the absence or presence of additional 1 mM SAM. (c) I_{612}/I_{460} ratiometric BRET signals of genetically encoded t-NLuc/P3 sensors in BL21 Star (DE3) cell lysates in the absence or presence of additional 100 μM ppGpp. t-NLuc/TAR (without the Pepper unit) acted as a negative control and the t-NLuc/S6 construct acted as a positive control. The measurement was performed at 25 °C in the presence of 5 μM HBC620 right after adding the 1% (v/v) furimazine substrate. (d, e) Bright field and fluorescence channel imaging of HEK-293T cells at 24 h after transfection with (d) mini-CMV-t-NLuc and pAV-U6+27-Tornado-TAR or with (e) mini-CMV-t-NLuc and pAV-U6+27-Tornado-S6. Fluorescence images were collected through a 593/20 nm filter after irradiation with a 561 nm laser at 25 °C in the presence of 5 μM HBC620. Scale bar, 20 μm. (f) I_{645}/I_{460} ratiometric signals of HEK-293T cells after confirming the successful transfection with mini-CMV-t-NLuc and pAV-U6+27-Tornado-TAR or pAV-U6+27-Tornado-S6. The measurement was performed in a plate reader at 25 °C in the presence of 5 μM HBC620 at 30 s after adding 1% (v/v) furimazine substrate. Shown are the mean and SD values from three independent replicates. *p < 0.05, ***p < 0.001 in two-tailed Student's t-test

selectivity of the riboswitches is maintained in these t-NLuc/RNA-based BRET sensors. Altogether, these above results indicated that by simply changing the aptamer domain, RNA-based BRET sensors can be modularly developed to allow detection of various target analytes.

Live-Cell Detection with Genetically Encoded RNA-Based BRET Sensors. We next asked if these t-NLuc/S6-based BRET sensors can be genetically encoded for intracellular measurement. We first cloned S6 and t-NLuc into a pETDuet vector to allow the coexpression of S6 RNA and the t-NLuc protein under two separate T7 promoters. As a control, another pETDuet vector was engineered to express only t-NLuc. After transforming these two plasmids respectively into BL21 Star (DE3) *Escherichia coli* cells and incubating with HBC620 and furimazine, a strong donor bioluminescent signal at \sim 460 nm was clearly detected (Figure S6). However, a minimal I_{612} acceptor signal was shown in these t-NLuc/S6-expressing cells.

To solve this problem, we tried to change the relative cellular expression levels of S6 and t-NLuc. This is because, as shown in Figure 1c, an enhanced BRET efficiency can be observed with an increasing ratio of S6:t-NLuc. We thus decided to suppress the cellular expression of t-NLuc by placing it under a weaker lac promoter (in substitution of T7), while S6 continued to be expressed under a strong T7 promoter. This new expression system allows the generation of an increased S6:t-NLuc concentration ratio inside cells, and

indeed, in this case, much clearer cellular I_{612}/I_{460} BRET signals were observed (Figure S6). Meanwhile, cellular BRET signals can be immediately observed right after adding the furimazine substrate. There was a slow decrease in the BRET signals over time, but still, ~75% of maximum signals can be observed at ~4 min (Figure S6). Theoretically, the ratiometric BRET signals may be independent of the substrate concentration or reaction time. However, in our case, likely due to the rapid cellular degradation of furimazine or the S6:t-NLuc complex, a decay in the ratiometric signal was still observed. Some advanced live-cell substrates, *e.g.*, endurazine and vivazine, may be potentially useful to further increase the stability and duration of these cellular BRET signals.

Our next goal was to study the performance of RNA-based BRET sensors inside these living *E. coli* cells. Again, we engineered the vectors to coexpress lac promoter-regulated t-NLuc and T7 promoter-controlled RNA sensors. Vectors expressing the t-NLuc/T1 tetracycline sensor, t-NLuc/M1 SAM sensor, and t-NLuc/P3 (p)ppGpp sensor were separately prepared and then respectively transformed into BL21 Star (DE3) *E. coli* cells. We first tried to detect the cellular accumulation of tetracycline. In this experiment, after adding 100 μ M tetracycline, a ~3.4-fold enhancement in the I_{612}/I_{460} BRET signal was detected in the t-NLuc/T1-expressing cells (Figure 3a). The addition of 0.1–100 μ M tetracycline can be distinguished based on the cellular BRET signals. This

detection range was similar to that from in vitro characterizations (Figure 2b).

We next asked if the SAM- and ppGpp-targeting BRET sensors can indeed be used to detect these cellular endogenous analytes. We first treated the t-NLuc/M1-expressing E. coli cells with 1-50 mM of L-methionine, a precursor that facilitates the cellular synthesis of SAM.⁶⁵ Upon the addition of L-methionine, an up to 2.0-fold increase in the cellular BRET signal was observed (Figure 3b). We also applied the t-NLuc/P3-expressing BL21 Star (DE3) cells to measure variations in the cellular ppGpp levels under different nutritional conditions. These sensor-expressing E. coli cells were either cultured in a nutrient-rich medium containing casamino acids and glucose⁶⁶ or a nutrient-poor M9 minimal medium supplemented with serine hydroxamate to induce bacterial starvation.⁶⁷ Indeed, in the nutrient-poor condition, an around 2.0-fold increase in the BRET signal was observed, indicating the cellular generation of ppGpp as a stringent response (Figure 3c). All of these data validated that these RNA-based BRET sensors can be used for detecting target analytes in living cells.

Moreover, we further tested if these t-NLuc/RNA-based BRET signals are bright enough to be detectable using an IVIS SpectrumCT system, a widely used preclinical *in vivo* study instrument. Similar to the above bioluminescence results (based on the plate reader), target-induced BRET signals can be clearly detected using the IVIS SpectrumCT (Figure 3d–f). A 26–75% enhancement in the cellular ratiometric signals was shown after adding 100 $\mu\rm M$ tetracycline, 50 mM L-methionine, or 5 mM serine hydroxamate. These results indicated that these RNA-based BRET sensors have sufficient brightness that may be potentially used for *in vitro* or even *in vivo* studies of cellular target analytes.

It is also worth mentioning that these RNA-based BRET sensors can also function in cell lysates. For example, in the cell lysates of t-NLuc/T1-, t-NLuc/M1-, or t-NLuc/P3-expressing BL21 Star (DE3) cells, upon the addition of 100 μ M tetracycline, 1 mM SAM, or 100 μ M ppGpp, an approximately 119, 21, and 90% enhancement in the I_{612}/I_{460} ratiometric signals was observed (Figure 4a–c). Interestingly, the performance of these RNA-based BRET sensors in living bacterial cells is even superior to that in the cell lysates, which is probably due to the influence of cell lysates on RNA folding and/or the strength of TAR–Tat interactions.

Last, we also tested if our RNA-based BRET system can also be genetically encoded and function within mammalian cells. For this purpose, we transfected our S6 construct into HEK-293T cells using a previously reported "Tornado" expression system. This Tornado platform enables rapid intracellular RNA circularization and protects RNA inserts from exonuclease degradation to increase the cellular expression levels of RNA sensors. After validating the expression of sensors in the transfected HEK-293T cells (Figure 4d,e), the I_{645}/I_{460} ratiometric signals were compared between t-NLuc/TAR-and t-NLuc/S6-expressing cells. An \sim 6.9-fold increase in the BRET signal was observed in cells expressing t-NLuc/S6 (Figure 4f), demonstrating the feasibility and potential function of this RNA-based BRET system in living mammalian cells.

CONCLUSIONS

In this project, we developed the first genetically encoded RNA-based BRET sensors, which can be used for intracellular detection and imaging of different target analytes. On the basis of natural RNA-protein interactions, a luciferase enzyme donor and an FR aptamer acceptor were coupled together to form an effective BRET platform. Modular BRET sensors have been further engineered to detect antibiotics, metabolites, and signaling molecules in both living cells and cell lysates. Following similar design principles, we expect the potential development of modular bioluminescent sensors for a wide range of target species, including small molecules, ions, RNAs, and proteins.

Another potential application of these BRET sensors is for the study of cellular RNA-protein interactions. By replacing TAR-Tat with other RNA-protein pairs of interest, the BRET signals can function as a genetically encoded indicator to determine the strength and distribution of RNA-protein interactions in living biological systems. For example, NLuc can be placed at either the N- or C-terminus of the target protein as the BRET donor, while Pepper can be encoded at the 5'- or 3'-end or a middle loop region (as done in this study) in the target RNA as the BRET acceptor. However, some optimization in the relative orientation and distance between NLuc and Pepper is still likely needed to maximize the energy transfer efficiency. Meanwhile, the potential usage of these RNA-based BRET sensors for in vivo imaging and high-throughput screening of RNA-targeted drugs can also be anticipated. Indeed, these general and modular BRET sensors can be a great complementary tool to the existing fluorescent RNA assays.

On the other hand, we have to mention that the current dynamic range, efficiency, and signal duration of these RNA-based BRET sensors are still quite limited. More systematic studies are still needed to further optimize FR/dye and luciferase/substrate pairs with better-matched wavelength, brightness, cellular stability, and relative orientation. Nevertheless, this current study has now opened the door for new functions of RNA molecules and nanodevices. A wide variety of designs and applications of RNA sensors can be expected in this emerging field.

ASSOCIATED CONTENT

Supporting Information

The Supporting Information is available free of charge at https://pubs.acs.org/doi/10.1021/acssensors.2c02213.

Fluorescence signals and bioluminescence spectra of the t-NLuc/TAR-Pepper construct; effect of incubation time and substrate concentration on the t-NLuc/S6 BRET signal; effect of Mg²⁺ concentration on the t-NLuc/S6 BRET signal; effect of the buffer condition on the BRET and fluorescence signal of the t-NLuc/S6 construct; fluorescence and BRET signals of different tetracycline, SAM, and ppGpp sensors; and effect of induction time and promoter on the cellular BRET signal (PDF)

AUTHOR INFORMATION

Corresponding Authors

Kewei Ren – Department of Chemistry, University of Massachusetts, Amherst, Massachusetts 01003, United States; School of Chemistry and Chemical Engineering, Nanjing University of Science and Technology, Nanjing 210094, China; Email: kwren@njust.edu.cn

Mingxu You — Department of Chemistry, University of Massachusetts, Amherst, Massachusetts 01003, United States; Molecular and Cellular Biology Program, University of Massachusetts, Amherst, Massachusetts 01003, United States; oorcid.org/0000-0003-3293-9760;

Email: mingxuyou@umass.edu

Authors

Lan Mi – Department of Chemistry, University of
 Massachusetts, Amherst, Massachusetts 01003, United States
 Qikun Yu – Department of Chemistry, University of
 Massachusetts, Amherst, Massachusetts 01003, United States

Aruni P. K. K. Karunanayake Mudiyanselage — Department of Chemistry, University of Massachusetts, Amherst, Massachusetts 01003, United States

Rigumula Wu – Department of Chemistry, University of Massachusetts, Amherst, Massachusetts 01003, United States Zhining Sun – Department of Chemistry, University of Massachusetts, Amherst, Massachusetts 01003, United

Ru Zheng – Department of Chemistry, University of Massachusetts, Amherst, Massachusetts 01003, United States

Complete contact information is available at: https://pubs.acs.org/10.1021/acssensors.2c02213

States; orcid.org/0000-0003-0358-960X

Author Contributions

L.M. and Q.Y. contributed equally. Q.Y., K.R., and M.Y. designed the experiments. L.M. and Q.Y. performed the majority of the experiments and analyzed the data. A.P.K.K.K.M. synthesized and purified the t-NLuc protein. R.W., Z.S., and R.Z. synthesized and characterized some RNA sensors. K.R. and M.Y. supervised the whole project. L.M. and M.Y. wrote the manuscript. All of the authors discussed the result shown in the manuscript.

Notes

The authors declare no competing financial interest.

ACKNOWLEDGMENTS

The authors gratefully acknowledge the support from an NSF CAREER award, the Alfred P. Sloan Research Fellowship, the Camille Dreyfus Teacher-Scholar Award, and the UMass Amherst start-up grant to M.Y. Q.Y. and R.Z. were also supported by NIH T32GM139789. We are grateful to Dr. James Chambers for the assistance in fluorescence imaging. The mini-CMV-Nluc-tDeg plasmid was a gift from Prof. Samie R. Jaffrey. The authors also thank other members in the You Lab for useful discussion and valuable comments.

REFERENCES

- (1) Greenwald, E. C.; Mehta, S.; Zhang, J. Genetically encoded fluorescent biosensors illuminate the spatiotemporal regulation of signaling networks. *Chem. Rev.* **2018**, *118*, 11707–11794.
- (2) Syed, A. J.; Anderson, J. C. Applications of bioluminescence in biotechnology and beyond. *Chem. Soc. Rev.* **2021**, *50*, 5668–5705.
- (3) Wilson, T.; Hastings, J. W. Bioluminescence. Curr. Rev. Cell Dev. Biol. 1998, 14, 197–230.
- (4) Ozawa, T.; Yoshimura, H.; Kim, S. B. Advances in fluorescence and bioluminescence imaging. *Anal. Chem.* **2013**, *85*, 590–609.
- (5) Zhou, X.; Mehta, S.; Zhang, J. Genetically encodable fluorescent and bioluminescent biosensors light up signaling networks. *Trends Biochem. Sci.* **2020**, *45*, 889–905.
- (6) Tantama, M.; Hung, Y. P.; Yellen, G. Imaging intracellular pH in live cells with a genetically encoded red fluorescent protein sensor. *J. Am. Chem. Soc.* **2011**, *133*, 10034–10037.
- (7) Dippel, A. B.; Anderson, W. A.; Park, J. H.; Yildiz, F. H.; Hammond, M. C. Development of ratiometric bioluminescent sensors

- for in vivo detection of bacterial signaling. ACS Chem. Biol. 2020, 15, 904–914.
- (8) Chen, T. W.; Wardill, T. J.; Sun, Y.; Pulver, S. R.; Renninger, S. L.; Baohan, A.; Schreiter, E. R.; Kerr, R. A.; Orger, M. B.; Jayaraman, V.; et al. Ultrasensitive fluorescent proteins for imaging neuronal activity. *Nature* **2013**, *499*, 295–300.
- (9) Griss, R.; Schena, A.; Reymond, L.; Patiny, L.; Werner, D.; Tinberg, C. E.; Baker, D.; Johnsson, K. Bioluminescent sensor proteins for point-of-care therapeutic drug monitoring. *Nat. Chem. Biol.* **2014**, *10*, 598–603.
- (10) Sun, Z.; Nguyen, T.; McAuliffe, K.; You, M. Intracellular Imaging with Genetically Encoded RNA-based Molecular Sensors. *Nanomaterials* **2019**, *9*, No. 233.
- (11) Yu, Q.; Ren, K.; You, M. Genetically encoded RNA nanodevices for cellular imaging and regulation. *Nanoscale* **2021**, *13*, 7988–8003.
- (12) Su, Y.; Hammond, M. C. RNA-based fluorescent biosensors for live cell imaging of small molecules and RNAs. *Curr. Opin. Biotechnol.* **2020**, *63*, 157–166.
- (13) Paige, J. S.; Nguyen-Duc, T.; Song, W.; Jaffrey, S. R. Fluorescence imaging of cellular metabolites with RNA. *Science* **2012**, 335, 1194.
- (14) Kellenberger, C. A.; Chen, C.; Whiteley, A. T.; Portnoy, D. A.; Hammond, M. C. RNA-based fluorescent biosensors for live cell imaging of second messenger cyclic di-AMP. *J. Am. Chem. Soc.* **2015**, 137, 6432–6435.
- (15) Wu, J.; Zaccara, S.; Khuperkar, D.; Kim, H.; Tanenbaum, M. E.; Jaffrey, S. R. Live imaging of mRNA using RNA-stabilized fluorogenic proteins. *Nat. Methods* **2019**, *16*, 862–865.
- (16) Griss, R.; Schena, A.; Reymond, L.; Patiny, L.; Werner, D.; Tinberg, C. E.; Baker, D.; Johnsson, K. Bioluminescent sensor proteins for point-of-care therapeutic drug monitoring. *Nat. Chem. Biol.* **2014**, *10*, 598–603.
- (17) Tenda, K.; van Gerven, B.; Arts, R.; Hiruta, Y.; Merkx, M.; Citterio, D. Paper-based antibody detection devices using bioluminescent BRET-switching sensor proteins. *Angew. Chem., Int. Ed.* **2018**, *57*, 15369–15373.
- (18) Liu, S.; Su, Y.; Lin, M. Z.; Ronald, J. A. Brightening up biology: advances in luciferase systems for in vivo imaging. *ACS Chem. Biol.* **2021**, *16*, 2707–2718.
- (19) Su, Y.; Walker, J. R.; Park, Y.; Smith, T. P.; Liu, L. X.; Hall, M. P.; Labanieh, L.; Hurst, R.; Wang, D. C.; Encell, L. P.; Kim, N.; Zhang, F.; Kay, M. A.; Casey, K. M.; Majzner, R. G.; Cochran, J. R.; Mackall, C. L.; Kirkland, T. A.; Lin, M. Z. Novel NanoLuc substrates enable bright two-population bioluminescence imaging in animals. *Nat. Methods* **2020**, *17*, 852–860.
- (20) Hall, M. P.; Unch, J.; Binkowski, B. F.; Valley, M. P.; Butler, B. L.; Wood, M. G.; Otto, P.; Zimmerman, K.; Vidugiris, G.; Machleidt, T.; Robers, M. B.; Benink, H. A.; Eggers, C. T.; Fan, F.; Encell, L. P.; Wood, K. V. Engineered luciferase reporter from a deep sea shrimp utilizing a novel imidazopyrazinone substrate. *ACS Chem. Biol.* **2012**, 7, 1848–1857.
- (21) England, C. G.; Ehlerding, E. B.; Cai, W. NanoLuc: a small luciferase is brightening up the field of bioluminescence. *Bioconjugate Chem.* **2016**, 27, 1175–1187.
- (22) Bouhedda, F.; Autour, A.; Ryckelynck, M. Light-up RNA aptamers and their cognate fluorogens: from their development to their applications. *Int. J. Mol. Sci.* **2018**, *19*, No. 44.
- (23) Paige, J.S.; Wu, K. Y.; Jaffrey, S. R. RNA mimics of green fluorescent protein. *Science* **2011**, 333, 642–646.
- (24) Song, W.; Strack, R. L.; Jaffrey, S. R. Imaging bacterial protein expression using genetically encoded RNA sensors. *Nat. Methods* **2013**, *10*, 873–878.
- (25) Kellenberger, C. A.; Wilson, S. C.; Sales-Lee, J.; Hammond, M. C. RNA-Based fluorescent biosensors for live cell imaging of second messengers cyclic di-GMP and cyclic AMP-GMP. *J. Am. Chem. Soc.* **2013**, *135*, 4906–4909.

- (26) You, M.; Litke, J. L.; Jaffrey, S. R. Imaging metabolite dynamics in living cells using a Spinach-based riboswitch. *Proc. Natl. Acad. Sci. U.S.A.* **2015**, *112*, E2756–E2765.
- (27) Porter, E. B.; Polaski, J. T.; Morck, M. M.; Batey, R. T. Recurrent RNA motifs as scaffolds for genetically encodable small-molecule biosensors. *Nat. Chem. Biol.* **2017**, *13*, 295–303.
- (28) Li, X.; Mo, L.; Litke, J. L.; Dey, S. K.; Suter, S. R.; Jaffrey, S. R. Imaging intracellular S-adenosyl methionine dynamics in live mammalian cells with a genetically encoded red fluorescent RNA-based sensor. *J. Am. Chem. Soc.* **2020**, *142*, 14117–14124.
- (29) Kim, H.; Jaffrey, S. R. A Fluorogenic RNA-based sensor activated by metabolite-induced RNA dimerization. *Cell Chem. Biol.* **2019**, *26*, 1725.e6–1731.e6.
- (30) Xu, Y.; Piston, D. W.; Johnson, C. H. A bioluminescence resonance energy transfer (BRET) system: application to interacting circadian clock proteins. *Proc. Natl. Acad. Sci. U.S.A.* **1999**, *96*, 151–156.
- (31) Pfleger, K. D. G.; Seeber, R. M.; Eidne, K. A. Bioluminescence resonance energy transfer (BRET) for the real-time detection of protein-protein interactions. *Nat. Protoc.* **2006**, *1*, 337–345.
- (32) Xu, X.; Souto, M.; Xie, Q.; Servick, S.; Subramanian, C.; von Arnim, A. G.; Johnson, C. H. Imaging protein interactions with bioluminescence resonance energy transfer (BRET) in plant and mammalian cells and tissues. *Proc. Natl. Acad. Sci. U.S.A.* **2007**, *104*, 10264–10269.
- (33) Dragulescu-Andrasi, A.; Chan, C. T.; De, A.; Massoud, T. F.; Gambhir, S. S. Bioluminescence resonance energy transfer (BRET) imaging of protein-protein interactions within deep tissues of living subjects. *Proc. Natl. Acad. Sci. U.S.A.* **2011**, *108*, 12060–12065.
- (34) Puglisi, J. D.; Chen, L.; Blanchard, S.; Frankel, A. D. Solution structure of a bovine immunodeficiency virus Tat-TAR peptide-RNA complex. *Science* **1995**, *270*, 1200–1203.
- (35) Ye, X.; Kumar, R. A.; Patel, D. J. Molecular recognition in the bovine immunodeficiency virus Tat peptide-TAR RNA complex. *Chem. Biol.* **1995**, *2*, 827–840.
- (36) Greenbaum, N. L. How Tat targets TAR: structure of the BIV peptide-RNA complex. *Structure* **1996**, *4*, 5–9.
- (37) Karn, J. Tackling Tat. J. Mol. Biol. 1999, 293, 235-254.
- (38) Selby, M. J.; Bain, E. S.; Luciw, P. A.; Peterlin, B. M. Structure, sequence, and position of the stem-loop in tar determine transcriptional elongation by tat through the HIV-1 long terminal repeat. *Genes Dev.* **1989**, *3*, 547–558.
- (39) D'Orso, I.; Frankel, A. D. RNA-mediated displacement of an inhibitory snRNP complex activates transcription elongation. *Nat. Struct. Mol. Biol.* **2010**, *17*, 815–821.
- (40) Puglisi, J. D.; Chen, L.; Blanchard, S.; Frankel, A. D. Solution structure of a bovine immunodeficiency virus Tat-TAR peptide-RNA complex. *Science* **1995**, 270, 1200–1203.
- (41) Roy, S.; Chen, C.; Rosen, C. A.; Sonenberg, N. A bulge structure in HIV-I TAR RNA is required for Tat binding and Tatmediated trans-activation. *Genes Dev.* **1990**, *4*, 1365–1373.
- (42) Filonov, G. S.; Jaffrey, S. R. RNA Imaging with dimeric Broccoli in live bacterial and mammalian cells. *Curr. Protoc. Chem. Biol.* **2016**, *8*, 1–28.
- (43) Trachman, R. J.; Demeshkina, N. A.; Lau, M. W. L.; Panchapakesan, S. S. S.; Jeng, S. C. Y.; Unrau, P. J.; Ferre-D'Amare, A. R. Structural basis for high-affinity fluorophore binding and activation by RNA Mango. *Nat. Chem. Biol.* **2017**, *13*, 807–813.
- (44) Dolgosheina, E. V.; Jeng, S. C.; Panchapakesan, S. S.; Cojocaru, R.; Chen, P. S.; Wilson, P. D.; Hawkins, N.; Wiggins, P. A.; Unrau, P. J. RNA Mango aptamer-fluorophore: a bright, high-affinity complex for RNA labeling and tracking. *ACS Chem. Biol.* **2014**, *9*, 2412–2420.
- (45) Chen, X.; Zhang, D.; Su, N.; Bao, B.; Xie, X.; Zuo, F.; Yang, L.; Wang, H.; Jiang, L.; Lin, Q.; et al. Visualizing RNA dynamics in live cells with bright and stable fluorescent RNAs. *Nat. Biotechnol.* **2019**, 37, 1287–1293.
- (46) Huang, K.; Chen, X.; Li, C.; Song, Q.; Li, H.; Zhu, L.; Yang, Y.; Ren, A. Structure-based investigation of fluorogenic Pepper aptamer. *Nat. Chem. Biol.* **2021**, *17*, 1289–1295.

- (47) Schulze-Gahmen, U.; Hurley, J. H. Structural mechanism for HIV-1 TAR loop recognition by Tat and the super elongation complex. *Proc. Natl. Acad. Sci. U.S.A.* **2018**, *115*, 12973–12978.
- (48) Romani, A. M. Cellular magnesium homeostasis. *Arch. Biochem. Biophys.* **2011**, *512*, 1–23.
- (49) Jahnen-Dechent, W.; Ketteler, M. Magnesium basics. Clin. Kidney J. 2012, 5, i3—i14.
- (50) Speer, B. S.; Shoemaker, N. B.; Salyers, A. A. Bacterial resistance to tetracycline: mechanisms, transfer, and clinical significance. *Clin. Microbiol. Rev.* **1992**, *5*, 387–399.
- (51) Wittmann, A.; Suess, B. Selection of tetracycline inducible self-cleaving ribozymes as synthetic devices for gene regulation in yeast. *Mol. Biosyst.* **2011**, *7*, 2419–2427.
- (52) Zuker, M. Mfold web server for nucleic acid folding and hybridization prediction. *Nucleic Acids Res.* **2003**, *31*, 3406–3415.
- (53) Holmes, N. E.; Charles, P. G. P. Safety and efficacy review of doxycycline. *Clin. Med.: Ther.* **2009**, *1*, 471–482.
- (54) Lu, S. C. S-Adenosylmethionine. *Int. J. Biochem. Cell Biol.* **2000**, 32, 391–395.
- (55) Papakostas, G. I.; Alpert, J. E.; Fava, M. S-adenosyl-methionine in depression: a comprehensive review of the literature. *Curr. Psychiatry Rep.* **2003**, *5*, 460–466.
- (56) Abranches, J.; Martinez, A. R.; Kajfasz, J. K.; Chavez, V.; Garsin, D. A.; Lemos, J. A. The molecular alarmone (p)ppGpp mediates stress responses, vancomycin tolerance, and virulence in Enterococcus faecalis. *J. Bacteriol.* **2009**, *191*, 2248–2256.
- (57) Haseltine, W. A.; Block, R. Synthesis of guanosine tetra- and pentaphosphate requires the presence of a codon-specific, uncharged transfer ribonucleic acid in the acceptor site of ribosomes. *Proc. Natl. Acad. Sci. U.S.A.* **1973**, *70*, 1564–1568.
- (58) Gallant, J.; Palmer, L.; Pao, C. C. Anomalous synthesis of ppGpp in growing cells. *Cell* 1977, 11, 181–185.
- (59) Loh, E.; Dussurget, O.; Gripenland, J.; Vaitkevicius, K.; Tiensuu, T.; Mandin, P.; Repoila, F.; Buchrieser, C.; Cossart, P.; Johansson, J. A trans-acting riboswitch controls expression of the virulence regulator PrfA in Listeria monocytogenes. *Cell* **2009**, *139*, 770–779.
- (60) Sherlock, M. E.; Sudarsan, N.; Breaker, R. R. Riboswitches for the alarmone ppGpp expand the collection of RNA-based signaling systems. *Proc. Natl. Acad. Sci. U.S.A.* **2018**, *115*, 6052–6057.
- (61) Peselis, A.; Serganov, A. ykkC riboswitches employ an add-on helix to adjust specificity for polyanionic ligands. *Nat. Chem. Biol.* **2018**, *14*, 887–894.
- (62) Sun, Z.; Wu, R.; Zhao, B.; Zeinert, R.; Chien, P.; You, M. Livecell imaging of guanosine tetra- and pentaphosphate (p)ppgpp with RNA-based fluorescent sensors. *Angew. Chem., Int. Ed.* **2021**, *60*, 24070–24074.
- (63) Ni, Y.; Rosier, B. J. H. M.; van Aalen, E. A.; Hanckmann, E. T. L.; Biewenga, L.; Makri Pistikou, A.; Timmermans, B.; Vu, C.; Roos, S.; Arts, R.; Li, W.; de Greef, T. F. A.; van Borren, M. M. G. J.; van Kuppeveld, F. J. M.; Bosch, B.; Merkx, M. A plug-and-play platform of ratiometric bioluminescent sensors for homogeneous immunoassays. *Nat. Commun.* 2021, 12, No. 4586.
- (64) Dale, N. C.; Johnstone, E. K. M.; White, C. W.; Pfleger, K. D. G. NanoBRET: the bright future of proximity-based assays. *Front. Bioeng. Biotechnol.* **2019**, *7*, No. 56.
- (65) Chu, J.; Qian, J.; Zhuang, Y.; Zhang, S.; Li, Y. Progress in the research of S-adenosyl-L-methionine production. *Appl. Microbiol. Biotechnol.* **2013**, 97, 41–49.
- (66) Hernandez, V. J.; Bremer, H. Guanosine tetraphosphate (ppGpp) dependence of the growth rate control of rrnB P1 promoter activity in *Escherichia coli*. *J. Biol. Chem.* **1990**, 265, 11605–11614.
- (67) Pizer, L. I.; Merlie, J. P. Effect of serine hydroxamate on phospholipid synthesis in *Escherichia coli*. *J. Bacteriol*. **1973**, 114, 980–987
- (68) Litke, J. L.; Jaffrey, S. R. Highly efficient expression of circular RNA aptamers in cells using autocatalytic transcripts. *Nat. Biotechnol.* **2019**, *37*, 667–675.